



CARDIOVASCULAR, PULMONARY, AND RENAL PATHOLOGY

Lipid Droplet Accumulation Is Associated with an Increase in Hyperglycemia-Induced Renal Damage

Prevention by Liver X Receptors

Eva Kiss,^{*†} Bettina Kränzlin,[‡] Katja Wagenblaß,^{*} Mahnaz Bonrouhi,^{*} Joachim Thiery,[§] Elisabeth Gröne,^{*} Viola Nordström,^{*} Daniel Teupser,[¶] Norbert Gretz,[‡] Ernst Malle,^{||} and Hermann-Josef Gröne^{*}

From the Department of Cellular and Molecular Pathology,^{*} German Cancer Research Center, Heidelberg, Germany; the Institute of Anatomy and Cell Biology,[†] and the Medical Research Center, Klinikum Mannheim,[‡] University of Heidelberg, Heidelberg, Germany; the Institute of Laboratory Medicine,[§] Clinical Chemistry and Molecular Diagnostics, University of Leipzig, Leipzig, Germany; the Institute of Laboratory Medicine,[¶] Ludwig-Maximilians-University Munich, Munich, Germany; and the Institute of Molecular Biology and Biochemistry,^{||} Center for Molecular Medicine, Medical University of Graz, Graz, Austria

Accepted for publication
November 19, 2012.

Address correspondence to
Hermann-Josef Gröne, M.D.,
or Eva Kiss, M.D., Department
of Cellular and Molecular
Pathology, German Cancer
Research Center (DKFZ), Im
Neuenheimer Feld 280, D-69120
Heidelberg, Germany. E-mail:
h.-j.groene@dkfz.de or e.kiss@dkfz.de.

Dyslipidemia is a frequent component of the metabolic disorder of diabetic patients contributing to organ damage. Herein, in low-density lipoprotein receptor-deficient hyperlipidemic and streptozotocin-induced diabetic mice, hyperglycemia and hyperlipidemia acted reciprocally, accentuating renal injury and altering renal function. In hyperglycemic-hyperlipidemic kidneys, the accumulation of Tip47-positive lipid droplets in glomeruli, tubular epithelia, and macrophages was accompanied by the concomitant presence of the oxidative stress markers xanthine oxidoreductase and nitrotyrosine, findings that could also be evidenced in renal biopsy samples of diabetic patients. As liver X receptors (LXR α , β) regulate genes linked to lipid and carbohydrate homeostasis and inhibit inflammatory gene expression in macrophages, the effects of systemic and macrophage-specific LXR activation were analyzed on renal damage in hyperlipidemic-hyperglycemic mice. LXR stimulation by GW3965 up-regulated genes involved in cholesterol efflux and down-regulated proinflammatory/profibrotic cytokines, inhibiting the pathomorphology of diabetic nephropathy, renal lipid accumulation, and improving renal function. Xanthine oxidoreductase and nitrotyrosine levels were reduced. In macrophages, GW3965 or LXR α overexpression significantly suppressed glycated or acetylated low-density lipoprotein-induced cytokines and reactive oxygen species. Specifically, in mice, transgenic expression of LXR α in macrophages significantly ameliorated hyperlipidemic-hyperglycemic nephropathy. The results demonstrate the presence of lipid droplet-induced oxidative mechanisms and the pathophysiologic role of macrophages in diabetic kidneys and indicate the potent regulatory role of LXRs in preventing renal damage in diabetes. (*Am J Pathol* 2013, 182: 727–741; <http://dx.doi.org/10.1016/j.ajpath.2012.11.033>)

Altered lipoprotein metabolism and intracellular accumulation of unsaturated free fatty acids, cholesteryl esters, and advanced lipoxidation/glyoxylation end products can accelerate the development and progression of glomerular and tubulointerstitial injury in patients with diabetes mellitus.^{1,2} Advanced lipoxidation/glyoxylation end products have been shown to induce expression of chemotactic factors [eg, monocyte chemoattractant protein-1 (MCP-1)] and adhesion molecules (eg, intercellular adhesion molecule 1) on endothelial, mesangial, and tubular epithelial cells, with consequent migration of monocytes/macrophages into the kidney.^{3–5} Growing

evidence indicates that macrophages accumulate in diabetic kidneys and contribute to the substantial inflammation and fibrosis that can be observed in diabetic nephropathy.⁶ Macrophages are cells at the intersection between lipid metabolism and inflammation.⁷ Excess lipids, through several signaling pathways (eg, NF- κ B), can activate macrophages, turn them into foam cells, and increase their production of inflammatory mediators.^{8,9} Specifically, data indicate

The work is supported by DFG (German Research Foundation) and SFB 938 (H.J.G. and S.P.).

intracellular lipid droplets as functionally active organelles with roles in cell signaling, regulation of lipid metabolism, and synthesis and secretion of inflammatory mediators¹⁰; reactive oxygen species (ROS), cytokines/chemokines (eg, IL-1 β and MCP-1), and growth factors (eg, platelet-derived growth factor and transforming growth factor β 1) then will induce profibrotic responses leading to organ loss.^{11–13}

Liver X receptors (LXRs) α and β are ligand-activated nuclear receptors. Both isoforms are expressed at high levels in macrophages.¹⁴ The renal expression of LXRs was found to be reduced in animal models of type 1 diabetes compared with healthy animals.¹⁵

After ligand binding, LXRs form heterodimers with retinoid X receptors and regulate transcription of genes involved in lipid/glucose metabolism and inflammation. Natural ligands of LXRs are derived from the oxidative metabolism of cholesterol (oxysterols), potentially implying that disorders of lipid metabolism influence the transcriptional activity of LXRs and may modulate inflammation.^{14,16} Previous studies have shown that LXRs control cholesterol efflux in macrophages inhibiting foam cell formation¹⁷ and reduce lipopolysaccharide-induced expression of inflammatory genes (eg, iNOS, COX2, IL-6). Furthermore, LXRs can prevent the development of atherosclerosis in different rodent models.^{18,19} Recently, we reported pronounced anti-inflammatory and antifibrotic effects of LXR activation in chronic renal allograft dysfunction and pointed to the substantial contribution of LXR-modulated inflammatory activity of macrophages in achieving these effects.²⁰

We sought to evaluate the effects of LXR activation by a specific synthetic agonist, GW3965, on the development of diabetic nephropathy and to dissect the contribution of macrophage LXR α . A mouse model of hyperlipidemia-aggravated hyperglycemia was taken as an animal model to mimic a metabolic state regularly present in patients with diabetes mellitus. To gain insight into the role of macrophages, mice specifically expressing LXR α in macrophages were studied. The concomitant presence of the oxidative stress markers xanthine oxidoreductase (XOR) and nitrotyrosine with tail-interacting protein of 47 kDa (Tip47)-positive lipid droplets could be shown in glomerular cells, tubular epithelia, and macrophages in kidneys of these hyperlipidemic-hyperglycemic mice and in renal biopsy samples of diabetic patients. These data, in congruence with the increased production of ROS and inflammatory/fibrotic mediators by lipid-loaded macrophages and tubular epithelial cells, provide insight into the mechanisms of intracellular lipid accumulation—mediated renal lesions, which can be effectively regulated by LXRs. The results demonstrate that LXR activation can prevent the development of hyperlipidemia/hyperglycemia-induced renal lesions by coordinated modulation of lipid metabolism and inflammation. The remarkable potency of LXR α in macrophages to protect kidneys from diabetic injury confirms the importance of the macrophage population in this renal disease and marks LXRs as *in vivo* relevant

modulators and therapeutic targets of macrophage functions in diabetic nephropathy.

Materials and Methods

Experimental Design

LDLR^{-/-} mice (C57BL/6 background; The Jackson Laboratory, Bar Harbor, ME) were crossed with mice with transgenic expression of LXR α in macrophages (C57BL/6 background, termed mLXR α -tg)²¹ to generate *LDLR*^{-/-} mLXR α -tg animals. Mice were initially maintained on a pelleted rodent chow diet, and at 7 weeks of age they were randomly assigned to one of the four diets: chow diet, Western diet (WD), chow + streptozotocin (STZ), and WD + STZ.

The experimental animal groups were as follows: *LDLR*^{-/-}, *LDLR*^{-/-} with GW3965, and *LDLR*^{-/-} mLXR α -tg (Table 1). In addition, mLXR α -tg mice and C57BL/6 wild-type (WT) mice were evaluated as control animals and are listed in Supplemental Table S1.

Rodent chow diet contained 4% fat, 24% protein, and 4.5% crude fiber (8604 Teklad rodent diet; Harlan Laboratories, Indianapolis, IN). The WD contained 21% fat and 0.15% cholesterol (TD 88137 Teklad custom research diet; Harlan Laboratories). The synthetic LXR agonist GW3965 (Sigma-Aldrich, Schnellendorf, Germany, and partly synthesized according to the method of Collins et al²²) was mixed into rodent chow diet or WD, and mice received 20 mg/kg body weight per day. The diets were fed for 20 weeks. Hyperglycemia was induced by 40 mg/kg body weight i.p. injection of the islet toxin STZ for 5 consecutive days at 7 and 9 weeks of age. The non-STZ groups were injected with citrate buffer as controls. All the animals had free access to tap water. Animal experiments were performed according to German laws on animal protection.

Histologic/Morphometric Analysis

Mice were sacrificed by cervical dislocation, and whole animals were perfused with PBS (pH 7.4) via the left ventricle. Kidneys were cut into 1-mm coronal slices and were fixed in 4% formaldehyde in PBS or zinc solution for histologic and immunohistologic analyses and in Karnovsky's solution [2% paraformaldehyde and 2.5% glutaraldehyde in 0.2 mol/L sodium cacodylate buffer (pH 7.2)] for electron microscopy. In addition, tissue slices were snap frozen in liquid nitrogen and were stored at -80°C.

Morphometric analysis was performed using a semi-automatic image analyzing system (Leica Q600 Qwin; Leica Microsystems, Cambridge, UK). Mesangial matrix increase was determined on PAS-stained 3- μ m kidney slices (50 glomeruli per slice) by the point-counting method. Results were expressed as a fraction of glomerular surface area.²³ Interstitial scarred area was quantified in Masson's trichrome-stained kidney slices. Ten randomly selected fields (100 \times) of cortex and outer medulla were evaluated. Results

Table 1 Biochemical Data in the Experimental Groups

Group	BW (g)	Kidney/BW ratio (%)	Plasma glucose (mg/dL)	Plasma cholesterol (mg/dL)	Plasma triglyceride (mg/dL)
1. <i>LDLR</i> ^{-/-}					
1a. Chow (n = 6)	30.8 ± 1.5	0.59 ± 0.01	196.7 ± 8.2	456.5 ± 52.2	192.7 ± 15.7
1b. WD (n = 6)	39.1 ± 1.9* vs 1a	0.62 ± 0.06	229.8 ± 17.3	1075.0 ± 128.8 [†] vs 1a	277.3 ± 92.5
1c. Chow + STZ (n = 8)	27.1 ± 0.6* vs 1a, [†] vs 1b	0.68 ± 0.02 [†] vs 1a	410.7 ± 55.9 [†] vs 1a, 1b	602.2 ± 59.9	205.0 ± 20.3
1d. WD + STZ (n = 6)	24.1 ± 0.9* vs 1a, 1b	0.83 ± 0.10 vs 1a	403.6 ± 55.6 [†] vs 1a, 1b	1514.0 ± 182.7 [†] vs 1a, 1c	377.0 ± 103.7* vs 1a
2. <i>LDLR</i> ^{-/-} + GW3965					
2a. Chow (n = 4)	31.4 ± 0.6	0.60 ± 0.01	234.8 ± 11.5	438.5 ± 21.7	468.3 ± 45.6 [†] vs 1a
2b. WD (n = 6)	31.6 ± 1.3* vs 1b	0.57 ± 0.02	233.7 ± 15.9	971.2 ± 268.6* vs 2a	279.4 ± 75.8
2c. Chow + STZ (n = 5)	24.9 ± 1.2* vs 2a, [†] vs 2b	0.69 ± 0.03	492.0 ± 71.7* vs 2a, 2b	445.5 ± 52.1	346.8 ± 90.4
2d. WD + STZ (n = 6)	25.5 ± 1.2 [†] vs 2a,* vs 2b	0.59 ± 0.03	403.0 ± 64.9* vs 2a, 2b	1205.0 ± 275.0 [†] vs 2a, 2c	361.7 ± 52.1
3. <i>LDLR</i> ^{-/-} mLXRa-tg					
3a. Chow (n = 6)	29.4 ± 0.9	0.58 ± 0.04	212.3 ± 6.9	296.7 ± 22.6* vs 1a, [†] vs 2a	130.2 ± 8.8 [†] vs 1a, 2a
3b. WD (n = 6)	34.2 ± 1.3* vs 3a	0.63 ± 0.03	207.3 ± 18.5	395.8 ± 64.1* vs 1b	133.8 ± 19.9
3c. Chow + STZ (n = 7)	22.2 ± 1.2 [†] vs 3a, 3b, 1c	0.77 ± 0.07	585.5 ± 95.7 [†] vs 3a, 3b	426.0 ± 23.4 [†] vs 3a	173.4 ± 29.4
3d. WD + STZ (n = 7)	25.4 ± 1.2* vs 3a, [†] vs 3b	0.78 ± 0.04* vs 3a	617.2 ± 12.6 [†] vs 3a, 3b, 1d,* vs 2d	1496.0 ± 235.0 [†] vs 3a,* vs 3b, 3c	345.3 ± 86.7

Data are given as means ± SEM.

**P* < 0.05.

[†]*P* < 0.01.

BW, body weight.

were expressed as a percentage of the total tubulointerstitial area, obtained after exclusion of glomeruli.²³

Foam cells were evaluated in 50 glomeruli according to the following classification: 0 (no foam cells), 0.5 to 1 (<25%), 1 (26% to 50%), 2 (51% to 75%), and 3 (>75% of the glomerular convolute). A final score was calculated as the sum of indices obtained by multiplication of the percentage of glomeruli with a respective degree of injury with the degree of injury (the percentage of glomeruli with 0.5 was multiplied by 0.5, that of degree 1 × 1, that of degree 2 × 2, and that of degree 3 × 3).²³ To judge the renal accumulation of neutral fat, frozen slices were stained with oil red O.

Electron Microscopy

The thickness of the glomerular basement membrane (GBM) was estimated using the orthogonal intercept method.^{24,25} Shortly, a subsample of the area of glomerular profiles (three glomeruli of a representative kidney slice per group) was photographed in a systematic independent manner, covering approximately 30% of the total profile area. A systematic line grid was superimposed over the electron microscopy micrographs. Where the grid lines transected the endothelial surface of the GBM, measurements were made of

the shortest distance between the endothelial plasma membrane and the plasma membrane of the podocyte foot processes, and a harmonic mean GBM thickness was calculated as described.^{24,25}

Immunohistochemical and Immunocytochemical Analysis

Immunohistochemical staining was done on sections of paraffin-embedded kidney samples. The following antibodies were used: rat anti-mouse monoclonal antibodies against F4/80 (Serotec, Oxford, UK), Mac-2/galectin-3 (Acris Antibodies GmbH, Hiddenhausen, Germany), CD3 (Santa Cruz Biotechnology, Santa Cruz, CA), polyclonal rabbit anti-mouse WT1 (C-19; Santa Cruz Biotechnology), and desmin (GeneTex Inc., San Antonio, TX) and mouse ascites fluid against α -smooth muscle actin (α -SMA; Sigma-Aldrich, St Louis, MO). An alkaline phosphatase/anti-alkaline phosphatase detection system was applied for the immune stainings (Dako, Hamburg, Germany). Control experiments were performed by omitting the primary antibody.

Positive glomerular cells were counted in ≥ 50 glomeruli and were given as the mean per glomerular slice; interstitial positive cells were counted in 20 high-power fields ($\times 40$) of

cortex and outer medulla and were recorded as mean per high-power field.

Polyclonal guinea pig antibodies recognizing Tip47, perlipin, and XOR purchased from Progen Biotechnik GmbH (Heidelberg, Germany), and rabbit antibody for nitrotyrosine epitopes (Millipore, Temecula, CA) were used on formalin-fixed mouse kidney slices and human kidney biopsy samples as well as formalin-fixed mouse peritoneal macrophages (4% paraformaldehyde; 5 minutes). The avidin-biotin complex detection method was applied. Staining intensities were evaluated semiquantitatively in whole mouse kidney slices or in 100 randomly chosen macrophages: 0, no staining; 1, mild staining; 2, moderate staining; and 3, strong staining, and a score was calculated as described for the evaluation of foam cells.

Isolation of Peritoneal Macrophages and Generation of Bone Marrow–Derived Macrophages

Peritoneal macrophages were collected with 10 mL of RPMI 1640 medium (Sigma-Aldrich, Taufkirchen, Germany) from male C57BL/6 (WT) and mLXR α -tg mice 72 hours after i.p. injection of 2 mL of thioglycolate (4%). Cells were seeded at 2×10^6 per well. After 12 hours of incubation at 37°C in 5% CO₂, the macrophages were thoroughly washed, and adherent cells were used for experiments. Purity was controlled by flow cytometry and Giemsa staining.

Generation of murine bone marrow–derived macrophages was performed according to standard protocols.^{26,27} In brief, mouse femurs were dissected, and each bone was flushed with 10 mL of PBS. A bone marrow cell suspension sample was collected and centrifuged. Pellets were resuspended in RPMI 1640 medium supplemented by 20% macrophage colony-stimulating factor—containing L929 medium. The cells were plated on non–tissue-culture-treated 10-cm Petri dishes and were incubated at 37°C in 5% CO₂. Fresh medium was provided on days 3 and 5, and the experiments were performed on day 7.

After preincubation with dimethyl sulfoxide or 3 μ mol/L GW3965 or 10 μ mol/L 22(R)-OH-cholesterol (Sigma-Aldrich, Taufkirchen, Germany) dissolved in dimethyl sulfoxide for 16 hours, macrophages were stimulated with 30 μ g/mL of glycated low-density lipoprotein (gLDL) or 50 μ g/mL of acetylated LDL (acLDL) for 12, 24, or 48 hours. The cells were then washed and collected for RNA isolation or were fixed on coverslips for 5 minutes with 4% paraformaldehyde for immunostaining.

Double Immunofluorescence Staining and Proximity Ligation Assay of Macrophages

Mouse peritoneal macrophages seeded onto coverslips and fixed with paraformaldehyde were blocked with 10% fetal calf serum/PBS 0.05% Tween and incubated with primary antibodies: rabbit- α Tip47 and goat- α XOR (both from Santa Cruz Biotechnology) for 1 hour at 37°C. After washing, they were stained with secondary antibodies (Alexa Fluor 488 and

546; Invitrogen, Darmstadt, Germany) (1 hour at 37°C). Cells were also stained with DAPI (Sigma-Aldrich, Taufkirchen, Germany) to visualize the nuclei. Negative controls were performed by omitting the primary antibody.

Proximity ligation assay, which allows visualization, localization, and quantification of individual protein interactions at a range of 30 to 40 nm, was performed according to the manufacturer's guidelines (Duolink orange detection system; Olink Bioscience, Uppsala, Sweden).²⁸ Formation of proximity ligation assay spots was analyzed by fluorescence microscopy (Zeiss Cell Observer; Carl Zeiss Micro-Imaging GmbH, Jena, Germany). Staining intensities were evaluated semiquantitatively in five randomly chosen fields ($\times 200$) (280 to 300 cells per group): 0, no staining; 0.5, moderate staining; and 1, strong staining, and a score was calculated as described for the evaluation of foam cells.

Detection of Intracellular ROS/Reactive Nitrogen Species in Macrophages and Tubular Epithelial Cells

ROS/reactive nitrogen species were detected using an ROS detection kit (Enzo Life Sciences, Lörrach, Germany) according to the manufacturer's instructions. This assay is designed to directly monitor real-time ROS/reactive nitrogen species production in live cells.²⁹ Peritoneal and bone marrow–derived macrophages (2×10^4 cells per well) and HK2 immortalized human proximal tubular cells (5×10^3 cells per well; ATCC, Manassas, VA) were seeded in black-walled 96-well plates and were treated as described previously herein. Plates were read after 10 and 60 minutes of stimulation with 50 μ g/mL of acLDL using a FLUOstar Optima multiwell plate fluorescent reader (BMG Labtech GmbH, Offenburg, Germany) equipped with a standard green (490/525 nm) and red (490/580 nm) filter (Optima Technologies, Atlanta, GA).

Real-Time RT-PCR

Total RNA was extracted from kidneys and cells using the method of Chomczynski and Sacchi³⁰ ($n = 4$ to 6 animals per group). RNA quality was checked using an RNA 6000 Nano Chip (Agilent Technologies, Waldbronn, Germany). Ten micrograms of total RNA was digested with DNase I according to the standard protocol. Three micrograms of total RNA (DNA free) was used for the first-strand cDNA synthesis using SuperScript II Reverse Transcriptase and oligo(dT)12-18 as primer (LifeTechnologies, Karlsruhe, Germany). Real-time PCR was performed by LightCycler using LightCycler-FastStart DNA Master SYBR green I kit (Roche Diagnostics, Mannheim, Germany) as described.²³ The primer sequences for target genes are shown in Table 2.

Biochemical Analysis

Plasma glucose levels (using retrobulbar venous plexus blood) were monitored every week (after induction of

Table 2 Sequences of Primers Used for Real-Time RT-PCR

Gene	Sense	Antisense
<i>GAPDH</i>	5'-ACTCCACTCTTCCACCTTC-3'	5'-GGTCCAGGGTTTCTTTACTCC-3'
<i>S18r</i>	5'-TGCCCTATCAACTTTTCGATGGTA-3'	5'-CAATTACAGGGCTCCAAAGAGT-3'
<i>RAGE</i>	5'-CCATCCTACCTTCTCCTG-3'	5'-AGCGACTATTCACCTTC-3'
<i>TNF-α</i>	5'-GCTTTCCGAATTCACCTGGAG-3'	5'-TTGCACCTCAGGGAAGAATC-3'
<i>MCP-1</i>	5'-ACCAAGCTCAAGAGAGAGG-3'	5'-ACATTCAAAGGTGCTGAAGAC-3'
<i>Collagen I</i>	5'-GAGCGGAGAGTACTGGATCG-3'	5'-GTTCGGGCTGATGTACCAGT-3'
<i>ABCA1</i>	5'-CCAGACAGTTGTGGATGTGG-3'	5'-GACCTCGCTCTTCCTTCCTT-3'
<i>ABCG1</i>	5'-CTTGCAGTAGGGCTTTTCAG-3'	5'-GCAAGGCTAGAGGTGTGGAG-3'
<i>SR-A1</i>	5'-GCACAGGATGCAGACAGAAA-3'	5'-TGGTCCATCTTGGTGACAGA-3'

hyperglycemia) using an Accu-Chek system (Roche Diagnostics). Continuous glucose levels higher than 250 mg/dL were considered diabetic. For measurements of renal functional parameters from blood and urine, animals were kept in metabolic cages for 24 hours. Levels of creatinine in serum and urine (enzymatic determination using the test kit Creatinine Plus Version 2 (Roche Diagnostics),³¹ urea nitrogen, total cholesterol, and triglycerides were analyzed using a Hitachi 9-17-E autoanalyzer (Hitachi, Frankfurt am Main, Germany). Albumin level in urine was measured by a competitive two-step enzyme immunoassay using as first antibody rabbit IgG to mouse albumin (MP Biomedicals, Santa Ana, CA).

Acetylation and Glycation of LDL

LDL ($d = 1.019$ to 1.063 g/mL) was isolated by sequential ultracentrifugation from plasma of normolipidemic human subjects as described.³² acLDL was prepared after treatment of native LDL by multiple 2- μ L aliquots of acetic anhydride.³² gLDL was prepared by incubating 1 mg/mL of LDL for 10 days at 37°C in Dulbecco's PBS (pH 7.4; without calcium and magnesium) that contained 100 μ mol/L EDTA and 25 mmol/L D-glucose.³³ EDTA was included in the buffer to inhibit metal-catalyzed oxidation reactions.

Statistical Analysis

All the data are presented as means \pm SEM. Data were analyzed for comparison of multiple *in vivo* experimental groups using analysis of variance (Bonferroni test). In addition, for *in vitro* experiments, the nonparametric *U*-test or unpaired *t*-test was applied as appropriate. A $P < 0.05$ was considered to show a significant difference between two groups.

Results

LXR Activation Improves Renal Function and Ameliorates Renal Pathomorphology in Hyperglycemic and/or Hyperlipidemic Mice

Biochemical data are presented in [Table 1](#) and [Supplemental Table S1](#). The STZ-induced increase in plasma glucose

levels was not significantly influenced by treatment with the LXR agonist ([Table 1](#)).

C57BL/6 WT mice did not develop evident hypercholesterolemia and hypertriglyceridemia when fed the WD and/or made diabetic with STZ ([Supplemental Table S1](#)). In contrast, *LDLR*^{-/-} mice fed the WD had high plasma cholesterol and triglyceride levels, and these values increased further when the mice were also diabetic. Hypertriglyceridemia, a known adverse effect of synthetic LXR agonists,³⁴ was observed in GW3965-treated groups when the animals were fed a standard chow diet; mice fed the WD did not show a further increase in plasma triglyceride levels when treated with GW3965 ([Table 1](#)).

Hyperlipidemia and hyperglycemia alone reduced creatinine clearance and increased urinary albumin excretion in *LDLR*^{-/-} mice; when combined, hyperlipidemia (WD) and hyperglycemia (STZ) aggravated renal functional parameters ([Figure 1A](#)). LXR activation by GW3965 led to evident preservation of renal function ([Figure 1A](#)).

Correspondingly, kidney morphology, moderately altered by either hyperlipidemia or hyperglycemia alone, was markedly altered by the combined stress of hyperlipidemia and hyperglycemia. Diabetic mice showed a significant increase in mesangial matrix compared with nondiabetic mice ($P < 0.01$ *LDLR*^{-/-} with STZ versus *LDLR*^{-/-}) ([Figure 1, B and C](#)). Glomeruli of mice fed the WD had occasional foam cell formation and fat droplets in the mesangium and some lipid deposition in tubular cells with occasional interstitial foam cells ([Figure 1, B and D](#)). A significant increase in mesangial matrix ($P < 0.05$ *LDLR*^{-/-} with STZ + WD versus *LDLR*^{-/-} + STZ), glomerular foam cells, and lipid tubular degeneration was found in hyperglycemic and hyperlipidemic animals (STZ + WD) ([Figure 1, B, C, and D](#)). Mesangial matrix increase and foam cell formation were significantly reduced in the respective GW3965-treated groups ([Figure 1, B, C, and D](#)).

Staining for the nuclear podocyte marker WT1 ([Figure 2, A and B](#)) and desmin ([Figure 2, C and D](#)), a marker of injured podocytes, demonstrated increased podocyte injury and loss in hyperlipidemic and/or hyperglycemic mice that could be partially prevented by GW3965 ([Figure 2](#)).

In hyperlipidemic and hyperglycemic mice, electron microscopy revealed thickened and irregular GBM, local foot process effacement of podocytes, endothelial cells without

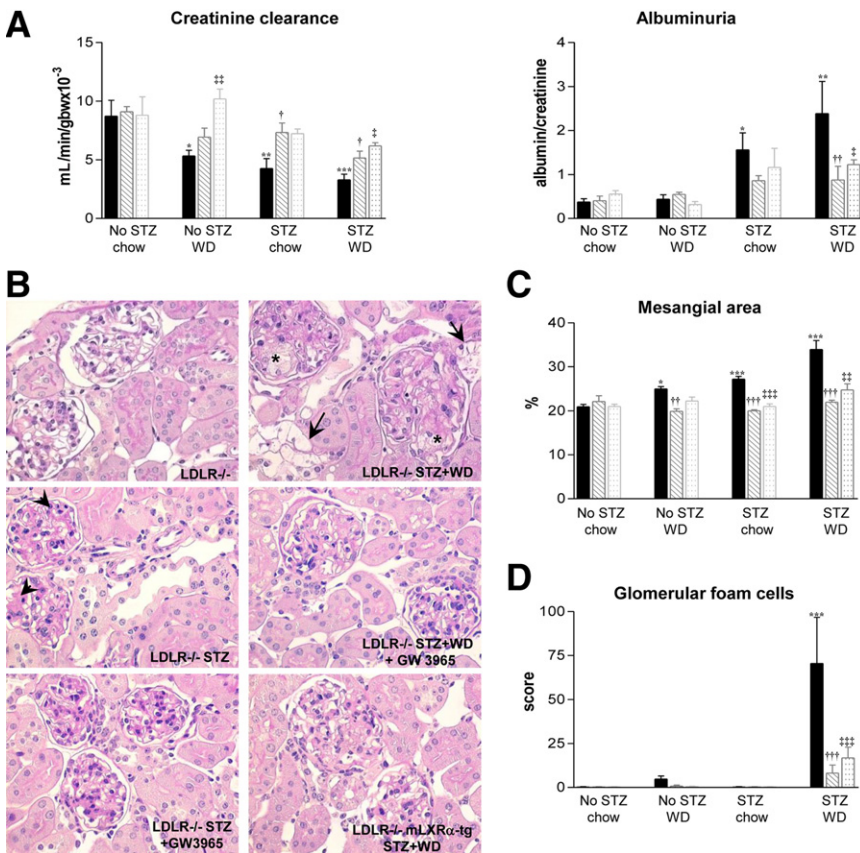


Figure 1 Excretory function and morphology of kidneys of hypertlipidemic, diabetic mice are preserved by LXR activation by GW3965 or macrophage-specific expression of LXR α (mLXR α -tg). Black bars indicate LDL^{-/-}; hashed bars indicate LDL^{-/-} + GW3965; dotted bars indicate LDL^{-/-} mLXR α -tg (A, C, and D). **A:** Creatinine clearance (left) and albuminuria (right) are presented for hyperlipidemic (WD), hyperglycemic (STZ), and hyperglycemic-hyperlipidemic (STZ + WD) mice without and with 20 mg/kg body weight GW3965 and for mice with overexpression of LXR α in macrophages, determined after 20 weeks of induction of diabetes and/or the start of the WD. **B:** PAS-stained kidney slices showing normal morphology in chow-fed LDL^{-/-} mice (LDL^{-/-}) mesangial matrix increase in diabetic (STZ) (arrowheads) and mesangial matrix increase with intraglomerular foam cells (asterisk) and fatty degeneration of tubules (arrows) in combined hypertlipidemic and hyperglycemic animals (STZ + WD). Treatment with GW3965 prevented mesangial matrix increase in diabetic mice (STZ + GW3965) and mesangial matrix increase and foam cell formation/tubular lipid degeneration in hyperlipidemic diabetic mice (STZ + WD + GW3965). A reduction in mesangial matrix increase and foam cell formation was also found in mLXR α -tg hypertlipidemic and hyperglycemic mice (mLXR α -tg + STZ + WD). Quantification of mesangial area (C) and glomerular foam cells (D) in different experimental groups. Values are expressed as means \pm SEM. * P < 0.05, ** P < 0.01, and *** P < 0.001 versus control LDL^{-/-}; † P < 0.05, †† P < 0.01, and ††† P < 0.001 treatment with GW3965 versus the respective LDL^{-/-} group without GW3965; ‡ P < 0.05, ‡‡ P < 0.01, and ‡‡‡ P < 0.001 mLXR α -tg versus the respective LDL^{-/-} group. Original magnification, \times 200 (B).

fenestrae, and lipid inclusions in the mesangium (Figure 3, A and D), indicating the involvement of all three glomerular cell types in the hyperlipidemia- and hyperglycemia-induced glomerular pathology. Tubular epithelia showed large amounts of lipid deposits (Figure 3G). The glomerular and tubular ultrastructural changes regressed with GW3965, supporting the protective effects on the glomerular (Figure 3, B, E, and I) and tubular (Figure 3H) integrity of LXR activation.

LXR Activation Reduces Lipid Accumulation and Modulates Genes of Lipid Metabolism in the Kidneys of Hyperlipidemic and Hyperglycemic-Hyperlipidemic Mice

Oil red O staining revealed an important accumulation of neutral lipids in kidneys of hyperlipidemic and hyperlipidemic-hyperglycemic LDL^{-/-} mice (Supplemental Figure S1), which correlated with higher expression of lipid droplet-associated proteins (Tip47 and perilipin) in these kidneys (Figure 4). Hyperglycemia alone was associated only with a discrete presence of lipid droplets in some glomeruli (Supplemental Figure S1). The members of the PAT (perilipin,

adipose differentiation-related protein, and Tip47) family of proteins have been characterized as structural leaflet constituents surrounding lipid droplets in different cell types.³⁵ The expression of Tip47 was localized to the mesangium, glomerular foam cells (Figure 4A), tubular epithelial cells, and macrophages in interstitium (Figure 4B). Perilipin expression was detected in glomerular foam cells (Supplemental Figure S2). GW3965 prevented renal lipid accumulation (Supplemental Figure S1) and reduced lipid droplet generation (Figure 4, A and C, and Supplemental Figure S2).

The intracellular accumulation of lipids and formation of lipid droplets may be caused by alterations in lipid uptake as well as synthesis and efflux. Therefore, the expression of genes intimately involved in various steps of cellular lipid metabolism was analyzed. Expression of mRNA for scavenger receptor class A 1, involved in the uptake of modified LDL, was down-regulated in kidneys of GW3965-treated hyperlipidemic-hyperglycemic animals (Figure 4D). Simultaneously, expression of ABCA1 and ABCG1 (implicated in cellular cholesterol efflux) as well as stearoyl CoA desaturase-1 (SCD-1) (known target genes of LXRs) was significantly up-regulated by GW3965 (Figure 4D).

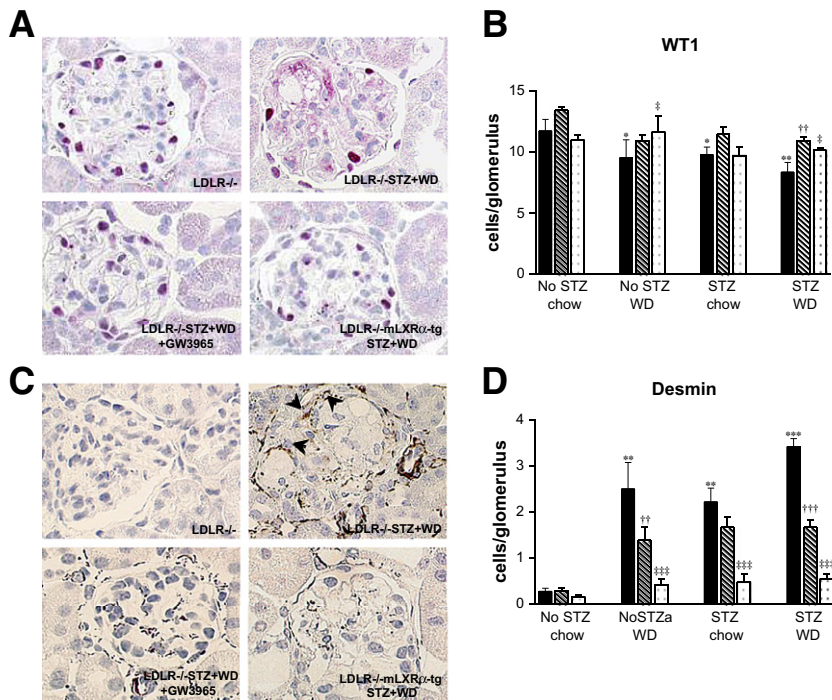


Figure 2 Less podocyte loss and injury by LXR activation by GW3965 or macrophage-specific expression of LXR α (mLXR α -tg) in hyperglycemic and/or hyperlipidemic mice. Black bars indicate LDLR^{-/-}; hashed bars indicate LDLR^{-/-} + GW3965; dotted bars indicate LDLR^{-/-} mLXR α -tg (B and D). Immunostaining for WT1 (A) and desmin (C) showing a decreased number of podocytes (WT1⁺) and an increased number of injured podocytes (desmin⁺) in glomeruli of hyperglycemic-hyperlipidemic LDLR^{-/-} mice (STZ + WD) (arrowheads, C); this was prevented by GW3965 or expression of LXR α in macrophages. Original magnification, $\times 400$. Quantification of WT1⁺ (B) and desmin⁺ (D) cells in different experimental groups. Values are expressed as means \pm SEM. * $P < 0.05$, ** $P < 0.01$, and *** $P < 0.001$ versus chow-fed LDLR^{-/-}; †† $P < 0.01$, ††† $P < 0.001$ treatment with GW3965 versus the respective LDLR^{-/-} group without GW3965; ‡ $P < 0.05$, ‡‡‡ $P < 0.001$ mLXR α -tg versus the respective LDLR^{-/-} group.

LXR Activation Reduces Oxidative Stress in the Kidneys of Hyperglycemic and/or Hyperlipidemic Mice

The biogenesis of lipid droplets is associated with the compartmentalization of lipid metabolic enzymes and other proteins (eg, kinases, small GTPases, and cytokines), indicating their potential function as intracellular signaling platforms.¹⁰ We previously identified XOR as an important enzyme for the production of ROS in hyperlipidemia-associated renal injury.^{36,37} Herein, we observed increased expression and a concomitant close association of the oxidative enzyme XOR and the oxidatively modified protein product nitrotyrosine with Tip47 in glomerular foam cells (Figure 4A), tubular epithelia, and interstitial macrophages (Figure 4B) in the hyperglycemic-hyperlipidemic mouse kidneys. The expression of XOR and nitrotyrosine was reduced in GW3965-treated kidneys (Figure 4, A–C), suggesting that the inhibition of lipid droplet generation and consequent reduction of lipid-related oxidative mechanisms might contribute to the protective effects of LXR activation.

LXR Activation Reduces Inflammation/Fibrosis and Modulates Expression of Inflammatory/Fibrotic Cytokines in Kidneys of Hyperglycemic and/or Hyperlipidemic Mice

Glomerular and interstitial mononuclear cells (Mac-2⁺ and F4/80⁺ macrophages, CD3⁺ T lymphocytes) were significantly increased when mice were exposed to hyperglycemia and hyperlipidemia and were remarkably decreased in kidneys of GW3965-treated mice (Figure 5, A–E).

Immunohistochemical analysis for Ki-67 showed a significantly increased proliferation rate of glomerular and tubulointerstitial cells by hyperlipidemia and/or hyperglycemia of LDLR^{-/-} mice; however, the overall number of proliferating cells was low. LXR stimulation with GW3965 had no effect on the proliferation rate of tubular epithelial cells (data not shown) but reduced significantly the proliferation of glomerular and interstitial cells (Supplemental Figure S3).

Focal fibrotic areas quantified in Masson's trichrome-stained kidney slices and α -SMA + glomerular and interstitial myofibroblasts, increased in diabetic and/or hyperlipidemic mice, showed a significant decrease in GW3965-treated groups (Figure 5, F–H).

In line with the morphometric analyses, the increased renal expression of the proinflammatory/profibrotic genes (receptor for advanced glycation end products, tumor necrosis factor α , MCP-1, transforming growth factor β 1) in hyperlipidemic-hyperglycemic LDLR^{-/-} mice was down-regulated by GW3965 (Figure 5I).

Effects of LXR Activation on Lipid Droplets, Oxidative Stress, and Inflammatory/Fibrotic Activity of Macrophages *in Vitro*

In macrophages, foam cell formation by acLDL was paralleled by increased expression of Tip47, XOR, and nitrotyrosine staining (Figure 6A and Supplemental Figure S4). GW3965 led to a reduced number of cells expressing Tip47, XOR, and nitrotyrosine (Figure 6A and Supplemental Figure S4). Macrophages overexpressing LXR α (mLXR α -tg) showed similar reactions without and with prestimulation

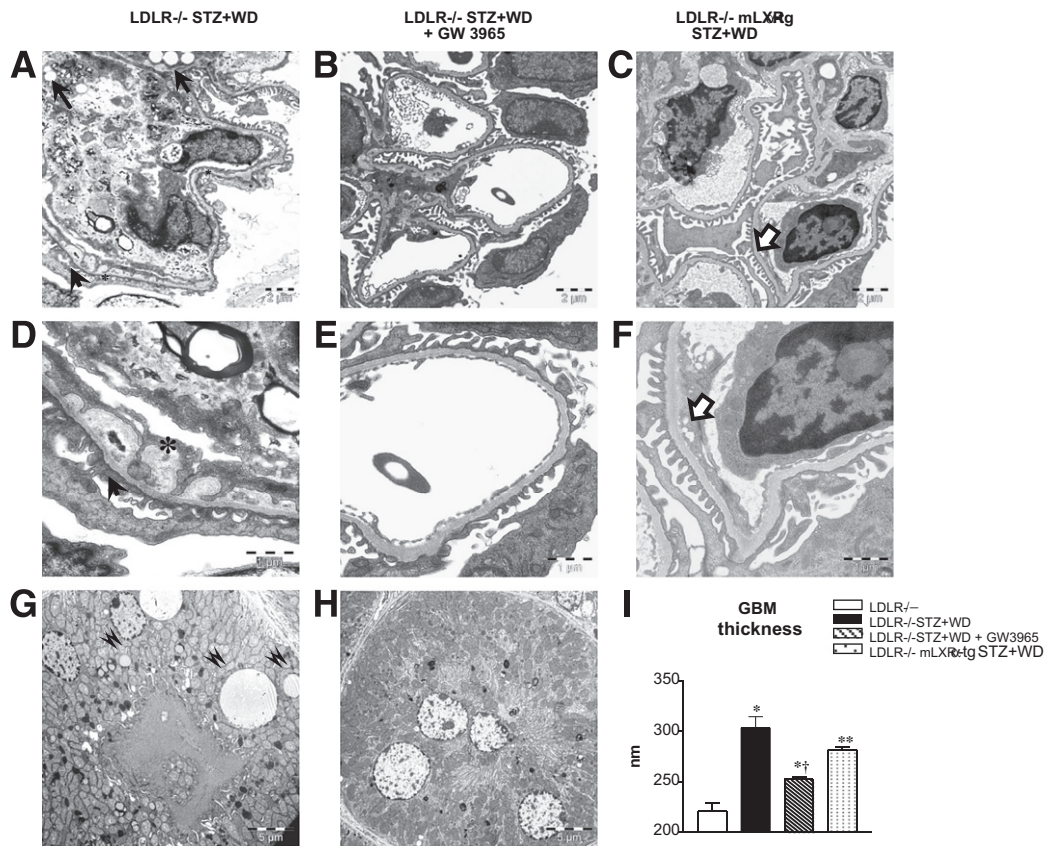


Figure 3 Electron microscopy confirms reduced podocyte, endothelial, and mesangial injury and evidences prevention of GBM thickening and lipid degeneration in glomerular and tubular epithelial cells by LXR activation. Glomerular capillary loop showing irregular thickening of the GBM, endothelial cells lacking fenestrae (**asterisks**), mesangial lipid droplets (**arrows**), and podocytes with effacement of foot processes (**arrowheads**) (**A** and **D**); tubular epithelia displaying a high number of intracellular lipids droplets (**double arrowheads**) (**G**) in an untreated hyperlipidemic-hyperglycemic mouse. Almost regular glomerular ultrastructure (**B** and **E**) and discrete lipid accumulation in tubular epithelial cells (**H**) of a GW3965-treated hyperlipidemic-hyperglycemic mouse. Glomerular capillary of a hyperlipidemic and hyperglycemic mLXR α -tg mouse showing only slight segmental thickening of the GBM and subendothelial lipid deposits (**open arrows**) (**C** and **F**). **D**, **E**, and **F** represent higher magnifications of **A**, **B**, and **C**, respectively. **I**: Graph showing the measured thickness of the GBM in different groups (see *Materials and Methods*). Values are expressed as means \pm SEM. * $P < 0.05$, ** $P < 0.01$ versus LDLR^{-/-}; † $P < 0.05$ treatment with versus without GW3965.

with the natural LXR ligand 22(R)-OH-cholesterol (**Figure 6A** and **Supplemental Figure S4**). Double immunofluorescence staining confirmed these data and showed the very close alignment of XOR to Tip47 + lipid droplets in lipid-loaded macrophages, a finding corroborated by proximity ligation assay (**Figure 6, B** and **D**). Exposure to acLDL increased ROS/reactive nitrogen species production of peritoneal and bone marrow–derived macrophages. ROS/reactive nitrogen species generation was reduced by pretreatment with GW3965 or transgene expression of LXR α (**Figure 6E** and data not shown). These results are in accord with our observations in human kidney tubular epithelial cells (HK2) (data not shown).

Next, macrophages were incubated with gLDL. Their inflammatory and fibrotic activity was investigated with and without LXR activation. Prestimulation of WT macrophages with GW3965 or 22(R)-OH-cholesterol reduced the expression of tumor necrosis factor α , MCP-1, collagen I, and receptor for advanced glycation end products compared with controls (**Figure 6F**). LXR α -tg macrophages, both without and with 22(R)-OH-cholesterol, also showed

diminished expression of these inflammatory and fibrotic genes when stimulated by gLDL (**Figure 6F**).

Expression of LXR α in Macrophages (mLXR α -tg) Is Sufficient to Prevent Deterioration of Renal Function and Morphology in Hyperglycemic and/or Hyperlipidemic Mice

Similar to LXR stimulation by GW3965, the hyperlipidemia- and hyperglycemia-induced decline in renal function (**Figure 1A**), impairment of glomerular damage (**Figure 1, B** and **C**), podocyte injury (**Figures 2** and **3, C** and **F**), and tubulointerstitial damage were significantly ameliorated in mLXR α -tg/LDLR^{-/-} animals (**Figure 1B**). The intrarenal mononuclear cell infiltrate was considerably reduced (**Figure 5, B, D, and E**) and could be associated with significantly lower expression of proinflammatory/profibrotic and oxidative genes (**Figure 5I**). The lower number of α -SMA⁺ interstitial cells and reduced scarred areas in

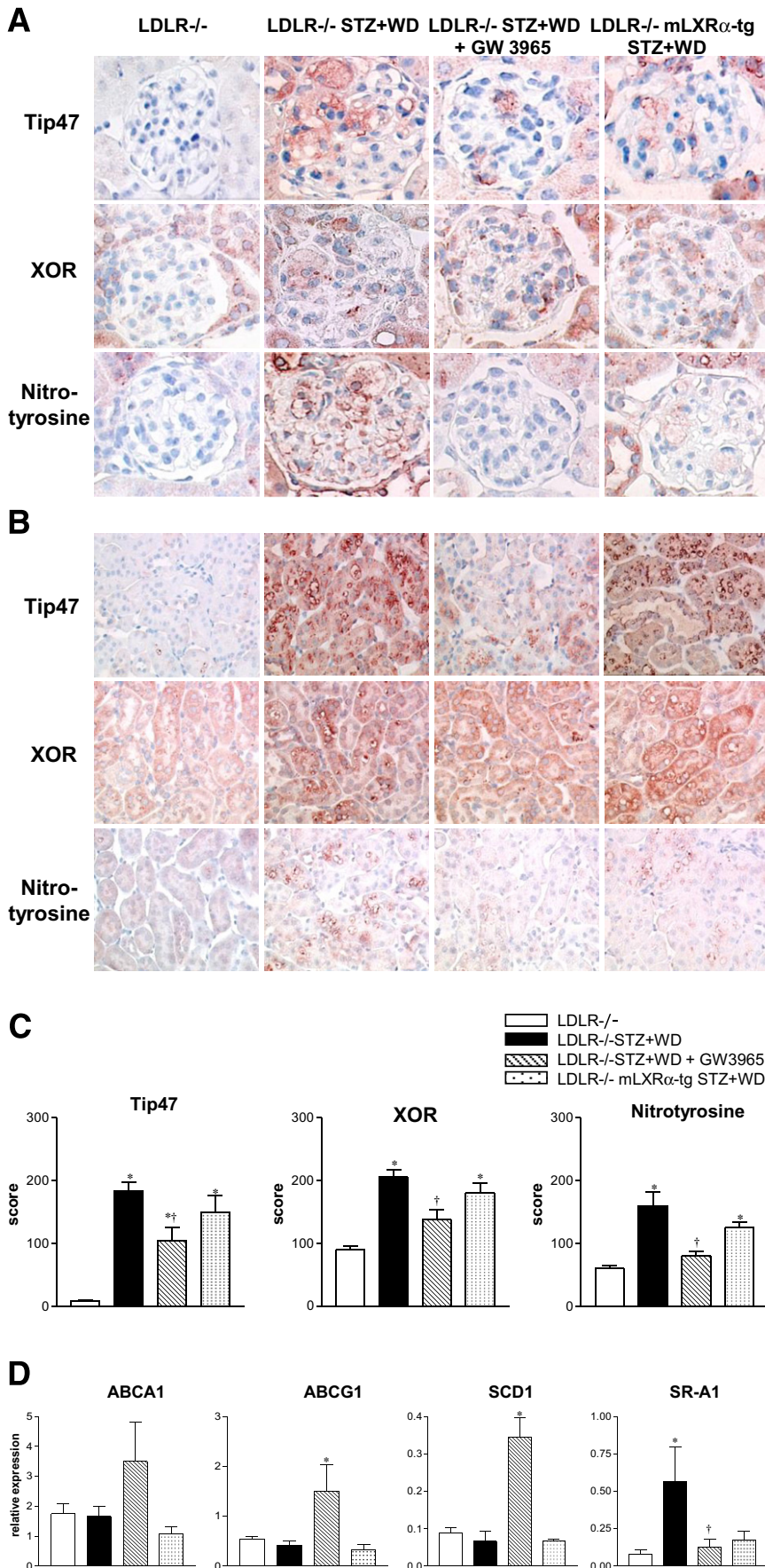


Figure 4 Lipid accumulation is associated with increased oxidative stress in kidneys of diabetic and hyperlipidemic mice and is reduced by LXR activation by GW3965 or macrophage-specific expression of LXR α (mLXR α -tg). Immunohistochemical analysis (alkaline phosphatase–anti-alkaline phosphatase) for the lipid droplet–associated protein Tip47, XOR, and nitrotyrosine in formalin-fixed kidney slices. Expression of Tip47 in the mesangium, glomerular foam cells (**A**), and tubular epithelial cells (mainly proximal but also some distal tubules and cortical collecting ducts) (**B**) of diabetic and hyperlipidemic mice (STZ + WD) are involved. XOR and nitrotyrosine are present in the tubular epithelia (**B**) of control kidneys (LDLR^{-/-}); expression is increased in hyperlipidemic and hyperglycemic kidneys and shows a similar expression pattern as Tip47. Weaker expression of Tip47, XOR, and nitrotyrosine is seen by GW3965 (glomerular and tubular) and mLXR α -tg (glomerular). Original magnification, $\times 400$. **C**: Graphs showing the staining scores (see *Materials and Methods*). Values are expressed as means \pm SEM ($n = 4$ to 5 animals per group). **D**: mRNA expression of genes related to cellular lipid metabolism in total kidney homogenates was determined by quantitative real-time PCR. Values are expressed as means \pm SEM. Values are normalized to GAPDH mRNA ($n = 4$ to 6 animals per group). * $P < 0.05$ versus LDLR^{-/-}; † $P < 0.05$ versus LDLR^{-/-} STZ + WD.

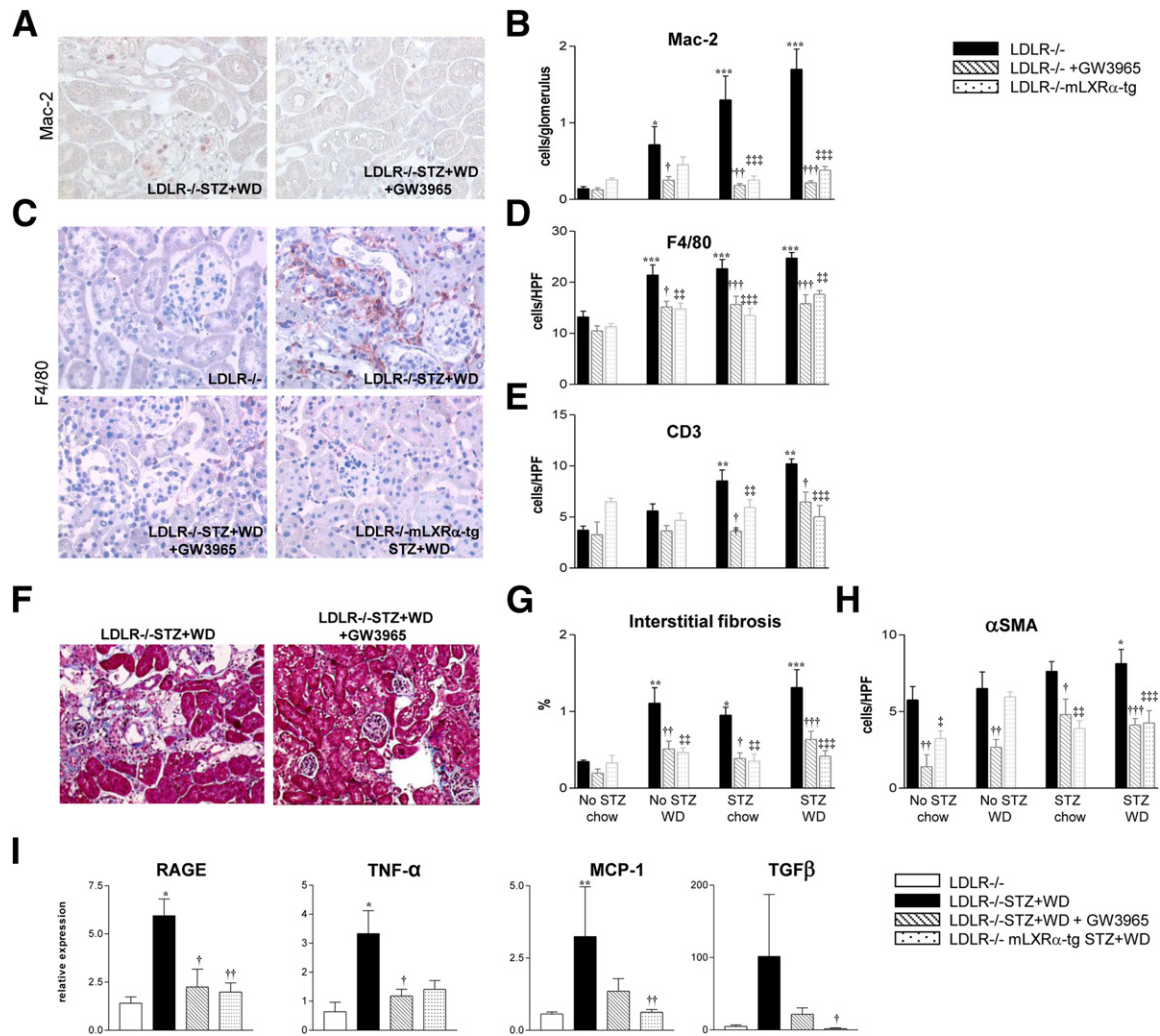


Figure 5 LXR activation by GW3965 or macrophage-specific expression of LXR α (mLXR α -tg) shows anti-inflammatory and antifibrotic effects in kidneys of diabetic mice. Reduced number of macrophages in glomeruli (Mac-2⁺) (A and B) and interstitium (F4/80⁺) (C and D) of GW3965-treated hyperglycemic-hyperlipidemic mice (STZ + WD + GW3965) and in mice with expression of LXR α in macrophages (mLXR α -tg) compared with untreated counterparts (STZ + WD). Original magnification: $\times 400$ (A); $\times 200$ (C). Quantification of Mac-2⁺ cells in glomeruli (50 glomeruli per slice) (B) and F4/80⁺ cells in interstitium [20 high power fields (HPF), 400 \times of cortex and outer medulla] (D). E: Quantification of the interstitial lymphocytic infiltrate (CD3⁺). F: Micrographs of representative kidney slices showing patchy fibrosis in hyperglycemic-hyperlipidemic LDLR^{-/-} mice (STZ + WD) and reduced fibrosis by treatment with GW3965 (STZ + WD + GW3965). Masson's trichrome; original magnification, $\times 200$. G: Fibrotic areas quantified morphometrically in Masson's trichrome-stained kidney slices. H: α -SMA⁺ myofibroblasts quantified in kidney interstitium. * $P < 0.05$, ** $P < 0.01$, and *** $P < 0.001$ versus LDLR^{-/-}; † $P < 0.05$, †† $P < 0.01$, and ††† $P < 0.001$ treatment with GW3965 versus the respective LDLR^{-/-} group without GW3965; ‡ $P < 0.01$, ‡‡ $P < 0.001$ mLXR α -tg versus the respective LDLR^{-/-} group. I: mRNA expression of genes related to inflammation and fibrosis in total kidney homogenates was determined by quantitative real-time PCR. * $P < 0.05$, ** $P < 0.01$ versus LDLR^{-/-}; † $P < 0.05$, †† $P < 0.01$ versus LDLR^{-/-} STZ + WD. Values are normalized to GAPDH mRNA ($n = 4$ to 6 animals per group). Values are expressed as means \pm SEM.

Masson's trichrome-stained kidney slices evidenced the antifibrotic actions of macrophage LXR α (Figure 5, G and H).

Oil red O staining showed reduced neutral lipid accumulation particularly in glomeruli and to a lesser degree in the tubulointerstitium of hyperlipidemic and hyperlipidemic-hyperglycemic mLXR α -tg/LDLR^{-/-} animals (Supplemental Figure S1). Immunohistochemical analysis for the lipid droplet-associated proteins supported these findings (Figure 4 and Supplemental Figure S2). Despite the elevated levels of ABCA1 and ABCG1 in LXR α -tg macrophages, as we have already shown,²¹ increased mRNA expression of these cholesterol efflux genes could not be detected in whole kidney

homogenates of transgenic mice (Figure 4D) compared with their chow diet-fed LDLR^{-/-} counterparts.

Correlation of the Experimental Data to Human Diabetic Nephropathy

Renal biopsy samples from patients with diabetic nephropathy with glomerular and tubular lipid deposits ($n = 8$), evidenced also in semithin slices and by transmission electron microscopy, were collected for immunohistochemical analyses. Clinical/laboratory data of these patients are provided in Supplemental Table S2. Expression of

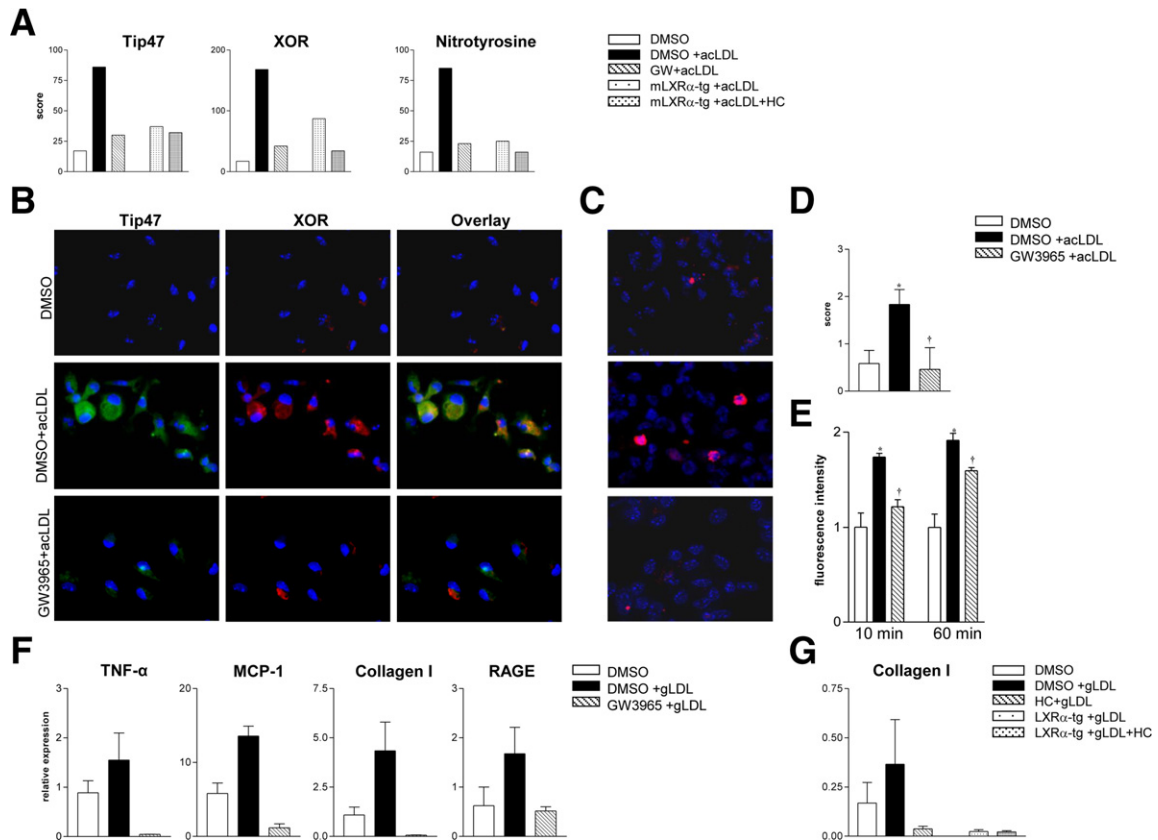


Figure 6 LXR activation coordinately modulates lipid metabolism, oxidative stress, and inflammatory/fibrotic activity of ac/gLDL-stimulated peritoneal macrophages. **A:** Expression of Tip47, XOR, and nitrotyrosine in mouse peritoneal macrophages incubated with 50 $\mu\text{g}/\text{mL}$ of acLDL for 24 hours. The number of cells expressing Tip47, XOR, and nitrotyrosine and their staining intensity were reduced when macrophages were prestimulated with GW3965 (3 $\mu\text{mol}/\text{L}$, 16 hours) and by LXR α -tg macrophages without and with prestimulation with 10 $\mu\text{mol}/\text{L}$ natural ligand 22(R)-OH-cholesterol for 16 hours. The graphs show the staining scores in different groups (one representative experiment of three). Corresponding micrographs are presented in [Supplemental Figure S4](#). **B:** Double immunofluorescence staining confirms the increased expression of XOR in lipid-loaded macrophages. A very close alignment of XOR to Tip47-positive lipid droplets in lipid-loaded macrophages can be observed. **C:** In addition, proximity ligation assay (PLA), which can visualize and quantify individual protein interactions in native cells using standard fluorescence microscopy, indicates a very close relation of XOR to lipid droplets in some lipid-loaded macrophages. **D:** Quantification of PLA spots in different groups (see *Materials and Methods*). **E:** ROS was measured in peritoneal macrophages (2×10^4 cells per well) after 10 and 60 minutes of stimulation with 50 $\mu\text{g}/\text{mL}$ of acLDL. The graph shows one representative experiment of three performed in quadruplicate. **F:** mRNA expression of genes related to oxidative stress, inflammation, and fibrosis in peritoneal macrophages stimulated with 30 $\mu\text{g}/\text{mL}$ of gLDL for 24 hours was reduced when the cells were pretreated with GW3965 (3 $\mu\text{mol}/\text{L}$) or 22(R)-OH-cholesterol (HC) (10 $\mu\text{mol}/\text{L}$) for 24 hours. One experiment of three, performed in duplicate. **G:** Reduced collagen I mRNA expression of gLDL stimulated LXR α -tg macrophages without and with HC (one experiment of three performed in duplicate). Values are normalized to S18r mRNA. Results are expressed as means \pm SEM. * $P < 0.05$ versus dimethyl sulfoxide (DMSO); $^{\dagger}P < 0.05$ with versus without GW3965.

Tip47 was observed as in kidneys of hyperlipidemic-hyperglycemic mice localizing focally and segmentally in mesangial areas, tubular epithelial cells, and interstitial mononuclear cells. As shown in [Figure 7](#), Tip47 expression was partly overlapping with the label for XOR and nitrotyrosine, suggesting a close association of lipid droplets with potential foci of oxidative processes in diabetic nephropathy.

Discussion

Clinical observations suggest that hyperlipidemia contributes to the progression of diabetic renal disease.^{2,38} Experimentally, it has been demonstrated that hyperlipidemia and hyperglycemia may act synergistically on the initiation and

progression of diabetic nephropathy.³⁹ We observed similar changes in kidneys of LDLR-deficient mice (C57BL6) when injected with STZ and fed the WD for 20 weeks. Under the combined stress of hyperglycemia and hyperlipidemia, mice developed complex renal damage: glomerular changes involving all three glomerular cell types, such as mesangial matrix increase and cell proliferation, thickened GBM, podocyte loss and injury, loss of endothelial fenestration and, seemingly, the result of hyperlipidemia, but accentuated by hyperglycemia, glomerular fat droplets, and foam cells; the fatty degeneration of the tubular epithelia was accompanied by a significant increase in interstitial macrophages and foam cells. These findings underscore the complexity and interrelatedness of pathogenic processes, which may play a role in the development of diabetic

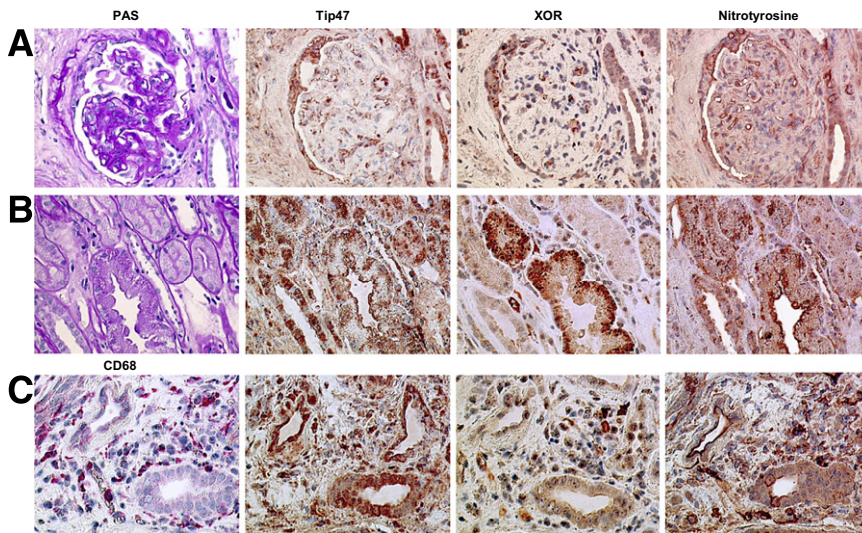


Figure 7 Expression of Tip47, XOR, and nitrotyrosine in renal biopsy samples of patients with diabetic nephropathy. Representative renal biopsy samples from a patient with biopsy-proven diabetic nephropathy with glomerular and tubular lipid deposits. Tip47 is expressed in the mesangial area of glomeruli (A), in tubular epithelial cells (B), and in interstitial macrophages (CD68⁺) (C). Focally, the expression of Tip47 is overlapping with the expression of XOR and nitrotyrosine including glomeruli (A), tubuli (B), and macrophages (C).

nephropathy. The addition of the synthetic nonselective LXR agonist GW3965 to the diet resulted in an important reduction of glomerular and tubulointerstitial changes and preservation of renal function (creatinine clearance and albuminuria). Correspondingly, herein, we observed accentuated kidney damage in diabetic *LDLR*^{-/-} mice on a high-fat diet for 5 months. With the synthetic, nonselective LXR agonist GW3965, an important reduction of glomerular and tubulointerstitial damage and preservation of renal function were achieved.

Treatment with LXR agonists in mice with type 2 diabetes has been found to decrease plasma glucose levels and hepatic glucose production by inhibiting key enzymes of gluconeogenesis.⁴⁰ In this model, we did not detect relevant differences in plasma glucose levels after STZ injections in the experimental groups with or without specific activation of LXRs. Thus, the beneficial effects of LXR activation by GW3965 on the development of diabetic nephropathy cannot be attributed to its plasma glucose-lowering effects.

Renal lipid and lipid droplets were significantly reduced in mice with LXR activation. LXRs are known to directly regulate expression of genes involved in lipid metabolism by binding of the LXR/retinoid X receptor heterodimer to respective response elements in the promoter region of target genes.¹⁶ Through induction of *ABCA1* and *ABCG1*, important lipid efflux genes, LXR activation might have contributed to the prevention of foam cell formation in macrophages and mesangial cells, as already observed *in vitro*,^{17,41} and to reduction of lipid accumulation in tubular epithelial cells. The relevance of this mechanism is supported by earlier findings demonstrating lipid accumulation in the kidney to be associated with reduced *ABCA1* expression in mesangial and tubular epithelial cells.^{42,43} In contrast, the reduced intrarenal expression of scavenger receptor class A1, a scavenger receptor involved in the uptake of oxidized LDL, is probably the result of the blunted inflammation in kidneys with LXR activation. Inflammatory cytokines (eg, IL-1 β) and

growth factors are known to contribute to the dysregulation of cellular lipid homeostasis by enhancing the expression of lipid influx pathways, particularly scavenger receptor class A and CD36, thereby accentuating intracellular lipid accumulation and foam cell formation.^{2,44} Thus, a coordinated decrease in lipid uptake and increase in lipid efflux pathways by LXRs might best explain the reduced amount of lipid droplets and foam cells in glomeruli and tubulointerstitium of GW3965-treated animals. This is relevant since studies have shown that renal lipid accumulation may accelerate glomerulosclerosis and interstitial fibrosis.^{45,46} Potential mechanisms include the direct effects of lipids on infiltrating and resident kidney cells, mainly by induction of oxidative stress, and the indirect effects of induced proinflammatory cytokines and growth factors, such as MCP-1 and transforming growth factor β 1.^{2,47} In previous studies, we identified XOR as an important enzyme involved in the increased ROS generation in hyperlipidemia-associated renal injury in rats.^{36,37} XOR can be an efficient source of superoxide anion radical that can react with NO to form peroxynitrite and to generate nitrotyrosylated proteins.⁴⁸ Plasma XOR activity has been found to be increased in diabetic mice and could be correlated with the degree of superoxide generation and could be normalized by allopurinol.⁴⁹ Increased formation of nitrotyrosine has also been demonstrated in diabetic kidneys.⁵⁰ As a sign of increased oxidative and nitrating stress, we found enhanced expression of XOR and epitopes for nitrotyrosine in kidneys of hyperglycemic and hyperlipidemic mice, which was reduced by LXR activation. Focally, a clear co-localization of both proteins with lipid droplet-associated proteins (Tip47 and perilipin) was seen in glomerular foam cells, tubular epithelia, and interstitial mononuclear cells (ie, macrophages). A similar expression pattern was found in renal biopsy samples of diabetic patients (Figure 7). Our observations were further supported by *in vitro* experiments in acLDL-loaded macrophages, and these findings are in accordance with recent data depicting

that overexpression of XOR in macrophages can exacerbate foam cell formation.⁵¹ In an earlier study, McManaman and coworkers⁵² localized XOR in the membrane of milk fat droplet membranes. By double immunofluorescence staining, we could provide evidence of a close alignment of XOR to Tip47-positive lipid droplets in lipid-loaded macrophages; this finding has been confirmed by a second method, namely, a positive proximity ligation assay result, hinting at a close (30 to 40 nm) association of these two proteins. Documenting the concomitant presence of an oxidative enzyme and its products with lipid droplets in renal resident and infiltrating cells, the present data point to a potential mechanism how intracellular lipids can be detrimental for the cell; foremost this can be prevented by LXR activation. In addition, we and others have shown that XOR can contribute to an increase of macrophage infiltration by induction of inflammatory cytokine and adhesion molecules.^{37,53,54}

In GW3965-treated hyperlipidemic-hyperglycemic mice, improved renal function and morphology was accompanied by a significantly diminished intrarenal mononuclear cell infiltrate and decreased renal expression of proinflammatory mediators (tumor necrosis factor α and MCP-1). The inflammatory activity (tumor necrosis factor α , MCP-1, and receptor for advanced glycation end products) of gLDL-stimulated macrophages pretreated with a synthetic or natural LXR ligand was reduced. The basic mechanism underlying the anti-inflammatory actions of LXRs has been shown to occur through the transrepression of NF- κ B signaling¹⁶ and consequent reduced transcription of cytokines and receptor for advanced glycation end products, one of the receptors of the advanced glycation end products.⁵⁵

Of note, LXR activation reduced renal expression of transforming growth factor β 1, the number of interstitial myofibroblasts, and the extent of fibrotic areas that correspond to the decreased collagen type I expression in GW3965-treated macrophages *in vitro*. These results are in line with earlier observations in kidney transplantation models in which LXR activation prevented the development of chronic renal allograft damage.²⁰ Recently, Beaven and coworkers⁵⁶ reported the suppression of fibrosis-related genes (eg, COL1A1) in primary mouse stellate cells by LXR ligands and increased liver fibrosis after injury in LXR $\alpha\beta$ -deficient mice.

Studies on human renal biopsy samples have shown that macrophage accumulation in diabetic kidneys correlates with serum creatinine levels, interstitial myofibroblast accumulation, and interstitial fibrosis.^{8,12,57} Thus, macrophage-mediated injury seems to be an important component in the development of diabetic nephropathy, which is not suppressed effectively by current therapies.⁶

Since in the kidney, LXR mRNA is expressed in all nephron segments, the protective effects of the nonselective LXR agonist GW3965 in hyperlipidemic-hyperglycemic kidneys may not be restricted to macrophages; the overall effect of the nonselective LXR agonist is likely to be a suppression of activity of infiltrating mononuclear cells and resident renal cells.

Nevertheless, transgenic expression of LXR α in macrophages was sufficient to prevent deterioration of renal function and morphology related to hyperglycemia and hyperlipidemia. Data concerning isoform-specific effects of LXRs are of practical interest for the generation of isoform-specific pharmacologic modulators, without potential adverse metabolic effects.

Activated macrophages can produce endogenous ligands of LXRs, eg, 24(S)-OH-cholesterol, 22(R)-OH-cholesterol, and 24(S),25-epoxycholesterol, which, in the state of constant expression of the receptor, apparently can lead to a biologically relevant activation without the need for further administration of an exogenous ligand.^{7,58,59} We previously demonstrated that macrophage transgenic expression of LXR α achieved by expression of the mouse LXR α cDNA under the control of a chicken lysozyme promoter resulted in activation of LXR α target genes, ABCA1 and ABCG1.²¹ The macrophage-restricted up-regulation of cholesterol efflux genes might explain the nonsignificant influence on lipid accumulation in tubular cells of mLXR α -tg mice compared with the GW3965-treated group. These experiments provide evidence for a robust capacity of the macrophage LXR α to inhibit diabetic nephropathy.

In summary, these findings demonstrate that lipid-induced oxidative mechanisms are operating in tissue injury of diabetic kidneys. Interrupting the pathophysiologic cascade of events induced by excess lipids and inhibiting inflammatory gene expression, LXR activation can prevent the development of diabetic nephropathy, even if aggravated by hyperlipidemia. Modulation of macrophage-mediated injury by LXRs seems to be relevant for efficient therapy.

Acknowledgments

We thank Claudia Schmidt, Gabi Schmidt, Sylvia Kaden, and Tjeerd Sijmonsma for expert technical help.

Supplemental Data

Supplemental material for this article can be found at <http://dx.doi.org/10.1016/j.ajpath.2012.11.033>.

References

- Jandeleit-Dahm K, Cao Z, Cox AJ, Kelly DJ, Gilbert RE, Cooper ME: Role of hyperlipidemia in progressive renal disease: focus on diabetic nephropathy. *Kidney Int Suppl* 1999, 71:S31–S36
- Abrass CK: Lipid metabolism and renal disease. *Contrib Nephrol* 2006, 151:106–121
- Kamanna VS, Pai R, Roh DD, Kirschenbaum MA: Oxidative modification of low-density lipoprotein enhances the murine mesangial cell cytokines associated with monocyte migration, differentiation, and proliferation. *Lab Invest* 1996, 74:1067–1079
- Gröne HJ, Walli AK, Gröne EF: The role of oxidatively modified lipoproteins in lipid nephropathy. *Contrib Nephrol* 1997, 120:160–175
- Kamanna VS, Pai R, Ha H, Kirschenbaum MA, Roh DD: Oxidized low-density lipoprotein stimulates monocyte adhesion to glomerular endothelial cells. *Kidney Int* 1999, 55:2192–2202

6. Tesch GH: Macrophages and diabetic nephropathy. *Semin Nephrol* 2010, 30:290–301
7. Shibata N, Glass CK: Macrophages, oxysterols and atherosclerosis. *Circ J* 2010, 74:2045–2051
8. Schmid H, Boucherot A, Yasuda Y, Henger A, Brunner B, Eichinger F, Nitsche A, Kiss E, Bleich M, Gröne HJ, Nelson PJ, Schlöndorff D, Cohen CD, Kretzler M: Modular activation of nuclear factor- κ B transcriptional programs in human diabetic nephropathy. *Diabetes* 2006, 55:2993–3003
9. Prieur X, Roszer T, Ricote M: Lipotoxicity in macrophages: evidence from diseases associated with the metabolic syndrome. *Biochim Biophys Acta* 2010, 1801:327–337
10. Bozza PT, Bandeira-Melo C: Mechanisms of leukocyte lipid body formation and function in inflammation. *Mem Inst Oswaldo Cruz* 2005, 1(Suppl):113–120
11. Zoja C, Garcia PB, Remuzzi G: The role of chemokines in progressive renal disease. *Front Biosci* 2009, 14:1815–1822
12. Yonemoto S, Machiguchi T, Nomura K, Minakata T, Nanno M, Yoshida H: Correlations of tissue macrophages and cytoskeletal protein expression with renal fibrosis in patients with diabetes mellitus. *Clin Exp Nephrol* 2006, 10:186–192
13. Vallon V, Thomson SC: Renal function in diabetic disease models: the tubular system in the pathophysiology of the diabetic kidney. *Annu Rev Physiol* 2012, 74:351–375
14. Repa JJ, Mangelsdorf DJ: The liver X receptor gene team: potential new players in atherosclerosis. *Nat Med* 2002, 8:1243–1248
15. Proctor G, Jiang T, Iwahashi M, Wang Z, Li J, Levi M: Regulation of renal fatty acid and cholesterol metabolism, inflammation, and fibrosis in akita and OVE26 mice with type 1 diabetes. *Diabetes* 2006, 55:2502–2509
16. Hong C, Tontonoz P: Coordination of inflammation and metabolism by PPAR and LXR nuclear receptors. *Curr Opin Genet Dev* 2008, 18:461–467
17. Larrede S, Quinn CM, Jessup W, Frisdal E, Olivier M, Hsieh V, Kim MJ, Van Eck M, Couvert P, Carrie A, Giral P, Chapman MJ, Guerin M, Le Goff W: Stimulation of cholesterol efflux by LXR agonists in cholesterol-loaded human macrophages is ABCA1-dependent but ABCG1-independent. *Arterioscler Thromb Vasc Biol* 2009, 29:1930–1936
18. Ogawa S, Lozach J, Benner C, Pascual G, Tangirala RK, Westin S, Hoffmann A, Subramaniam S, David M, Rosenfeld MG, Glass CK: Molecular determinants of crosstalk between nuclear receptors and toll-like receptors. *Cell* 2005, 122:707–721
19. Terasaka N, Hiroshima A, Koieyama T, Ubukata N, Morikawa Y, Nakai D, Inaba T: T-0901317, a synthetic liver X receptor ligand, inhibits development of atherosclerosis in LDL receptor-deficient mice. *FEBS Lett* 2003, 536:6–11
20. Kiss E, Popovic Z, Bedke J, Wang S, Bonrouhi M, Gretz N, Stettner P, Teupser D, Thiery J, Porubsky S, Adams J, Gröne HJ: Suppression of chronic damage in renal allografts by liver X receptor (LXR) activation: relevant contribution of macrophage LXR α . *Am J Pathol* 2011, 179:92–103
21. Teupser D, Kretzschmar D, Tennert C, Burkhardt R, Wilfert W, Fengler D, Naumann R, Sippel AE, Thiery J: Effect of macrophage overexpression of murine liver X receptor- α (LXR- α) on atherosclerosis in LDL-receptor deficient mice. *Arterioscler Thromb Vasc Biol* 2008, 28:2009–2015
22. Collins JL, Fivush AM, Watson MA, Galardi CM, Lewis MC, Moore LB, Parks DJ, Wilson JG, Tippin TK, Binz JG, Plunket KD, Morgan DG, Beaudet EJ, Whitney KD, Kliewer SA, Willson TM: Identification of a nonsteroidal liver X receptor agonist through parallel array synthesis of tertiary amines. *J Med Chem* 2002, 45:1963–1966
23. Adams J, Kiss E, Arroyo AB, Bonrouhi M, Sun Q, Li Z, Gretz N, Schnitger A, Zouboulis CC, Wiesel M, Wagner J, Nelson PJ, Gröne HJ: 13-*cis* retinoic acid inhibits development and progression of chronic allograft nephropathy. *Am J Pathol* 2005, 167:285–298
24. Hirose K, Osterby R, Nozawa M, Gundersen HJ: Development of glomerular lesions in experimental long-term diabetes in the rat. *Kidney Int* 1982, 21:689–695
25. Guo M, Ricardo SD, Deane JA, Shi M, Cullen-McEwen L, Bertram JF: A stereological study of the renal glomerular vasculature in the db/db mouse model of diabetic nephropathy. *J Anat* 2005, 207:813–821
26. Weischenfeldt J, Porse B: Bone marrow-derived macrophages (BMM): isolation and applications. *CSH Protoc* 2008. <http://dx.doi.org/10.1101/pdb.prot5080>
27. Gersuk GM, Razai LW, Marr KA: Methods of in vitro macrophage maturation confer variable inflammatory responses in association with altered expression of cell surface lectin-1. *J Immunol Methods* 2008, 329:157–166
28. Söderberg O, Gullberg M, Jarvius M, Ridderstråle K, Leuchowius KJ, Jarvius J, Wester K, Hydbring P, Bahram F, Larsson LG, Landegren U: Direct observation of individual endogenous protein complexes in situ by proximity ligation. *Nat Methods* 2006, 3:995–1000
29. Huo X, Juergens S, Zhang X, Rezaei D, Yu C, Strauch ED, Wang JY, Cheng E, Meyer F, Wang DH, Zhang Q, Spechler SJ, Souza RF: Deoxycholic acid causes DNA damage while inducing apoptotic resistance through NF- κ B activation in benign Barrett's epithelial cells. *Am J Physiol Gastrointest Liver Physiol* 2011, 301:G278–G286
30. Chomczynski P, Sacchi N: Single-step method of RNA isolation by acid guanidinium thiocyanate-phenol-chloroform extraction. *Anal Biochem* 1987, 162:156–159
31. Keppler A, Gretz N, Schmidt R, Kloetzer HM, Groene HJ, Lelongt B, Meyer M, Sadick M, Pill J: Plasma creatinine determination in mice and rats: an enzymatic method compares favorably with a high-performance liquid chromatography assay. *Kidney Int* 2007, 71:74–78
32. Malle E, Ibovnik A, Leis HJ, Kostner GM, Verhallen PF, Sattler W: Lysine modification of LDL or lipoprotein(a) by 4-hydroxynonenal or malondialdehyde decreases platelet serotonin secretion without affecting platelet aggregability and eicosanoid formation. *Arterioscler Thromb Vasc Biol* 1995, 15:377–384
33. Lamharzi N, Renard CB, Kramer F, Pennathur S, Heinecke JW, Chait A, Bornfeldt KE: Hyperlipidemia in concert with hyperglycemia stimulates the proliferation of macrophages in atherosclerotic lesions: potential role of glucose-oxidized LDL. *Diabetes* 2004, 53:3217–3225
34. Fiévet C, Staels B: Liver X receptor modulators: effects on lipid metabolism and potential use in the treatment of atherosclerosis. *Biochem Pharmacol* 2009, 77:1316–1327
35. Wolins NE, Brasaemle DL, Bickel PE: A proposed model of fat packaging by exchangeable lipid droplet proteins. *FEBS Lett* 2006, 580:5484–5491
36. Scheuer H, Gwinner W, Hohbach J, Gröne EF, Brandes RP, Malle E, Olbricht CJ, Walli AK, Gröne HJ: Oxidant stress in hyperlipidemia-induced renal damage. *Am J Physiol Renal Physiol* 2000, 278:F63–F74
37. Gwinner W, Scheuer H, Haller H, Brandes RP, Groene HJ: Pivotal role of xanthine oxidase in the initiation of tubulointerstitial renal injury in rats with hyperlipidemia. *Kidney Int* 2006, 69:481–487
38. Samuelsson O, Mulec H, Knight-Gibson C, Attman PO, Kron B, Larsson R, Weiss L, Wedel H, Alaupovic P: Lipoprotein abnormalities are associated with increased rate of progression of human chronic renal insufficiency. *Nephrol Dial Transplant* 1997, 12:1908–1915
39. Spencer MW, Mühlfeld AS, Segerer S, Hudkins KL, Kirk E, LeBoeuf RC, Alpers CE: Hyperglycemia and hyperlipidemia act synergistically to induce renal disease in LDL receptor-deficient BALB mice. *Am J Nephrol* 2004, 24:20–31
40. Steffensen KR, Gustafsson JA: Putative metabolic effects of the liver X receptor (LXR). *Diabetes* 2004, 53(Suppl 1):S36–S42
41. Wu J, Zhang Y, Wang N, Davis L, Yang G, Wang X, Zhu Y, Breyer MD, Guan Y: Liver X receptor- α mediates cholesterol efflux in glomerular mesangial cells. *Am J Physiol Renal Physiol* 2004, 287:F886–F895
42. Johnson AC, Yabu JM, Hanson S, Shah VO, Zager RA: Experimental glomerulopathy alters renal cortical cholesterol, SR-B1, ABCA1, and HMG CoA reductase expression. *Am J Pathol* 2003, 162:283–291
43. Takemura T, Yoshioka K, Aya N, Murakami K, Matumoto A, Itakura H, Kodama T, Suzuki H, Maki S: Apolipoproteins and

- lipoprotein receptors in glomeruli in human kidney disease. *Kidney Int* 1993, 43:918–927
44. Ruan XZ, Varghese Z, Moorhead JF: An update on the lipid nephrotoxicity hypothesis. *Nat Rev Nephrol* 2009, 5:713–721
 45. Gröne HJ, Hohbach J, Gröne EF: Modulation of glomerulosclerosis and interstitial fibrosis by native and modified lipoprotein. *Kidney Int Suppl* 1996, 49:S18–S22
 46. Sun L, Halaihel N, Zhang W, Rogers T, Levi M: Role of sterol regulatory element-binding protein 1 in regulation of renal lipid metabolism and glomerulosclerosis in diabetes mellitus. *J Biol Chem* 2002, 277:18919–18927
 47. Chow FY, Nikolic-Paterson DJ, Ozols E, Atkins RC, Rollin BJ, Tesch GH: Monocyte chemoattractant protein-1 promotes the development of diabetic renal injury in streptozotocin-treated mice. *Kidney Int* 2006, 69:73–80
 48. Godber BL, Doel JJ, Durgan J, Eisenthal R, Harrison R: A new route to peroxynitrite: a role for xanthine oxidoreductase. *FEBS Lett* 2000, 475:93–96
 49. Matsumoto S, Koshiishi I, Inoguchi T, Nawata H, Utsumi H: Confirmation of superoxide generation via xanthine oxidase in streptozotocin-induced diabetic mice. *Free Radic Res* 2003, 37:767–772
 50. Fujii H, Kono K, Nakai K, Goto S, Komaba H, Hamada Y, Shinohara M, Kitazawa R, Kitazawa S, Fukagawa M: Oxidative and nitrosative stress and progression of diabetic nephropathy in type 2 diabetes. *Am J Nephrol* 2010, 31:342–352
 51. Kushiyama A, Okubo H, Sakoda H, Kikuchi T, Fujishiro M, Sato H, Kushiyama S, Iwashita M, Nishimura F, Fukushima T, Nakatsu Y, Kamata H, Kawazu S, Higashi Y, Kurihara H, Asano T: Xanthine oxidoreductase is involved in macrophage foam cell formation and atherosclerosis development. *Arterioscler Thromb Vasc Biol* 2012, 32:291–298
 52. McManaman JL, Palmer CA, Wright RM, Neville MC: Functional regulation of xanthine oxidoreductase expression and localization in the mouse mammary gland: evidence of a role in lipid secretion. *J Physiol* 2002, 545:567–579
 53. Sun K, Kiss E, Bedke J, Stojanovic T, Li Y, Gwinner W, Gröne HJ: Role of xanthine oxidoreductase in experimental acute renal-allograft rejection. *Transplantation* 2004, 77:1683–1692
 54. Gibbings S, Elkins ND, Fitzgerald H, Tiao J, Weyman ME, Shibao G, Fini MA, Wright RM: Xanthine oxidoreductase promotes the inflammatory state of mononuclear phagocytes through effects on chemokine expression, peroxisome proliferator-activated receptor- γ sumoylation, and HIF-1 α . *J Biol Chem* 2011, 286:961–975
 55. Li J, Schmidt AM: Characterization and functional analysis of the promoter of RAGE, the receptor for advanced glycation end products. *J Biol Chem* 1997, 272:16498–16506
 56. Beaven SW, Wroblewski K, Wang J, Hong C, Bensinger S, Tsukamoto H, Tontonoz P: Liver X receptor signaling is a determinant of stellate cell activation and susceptibility to fibrotic liver disease. *Gastroenterology* 2011, 140:1052–1062
 57. Nguyen D, Ping F, Mu W, Hill P, Atkins RC, Chadban SJ: Macrophage accumulation in human progressive diabetic nephropathy. *Nephrology (Carlton)* 2006, 11:226–231
 58. Hultén LM, Lindmark H, Diczfalusy U, Björkhem I, Ottosson M, Liu Y, Bondjers G, Wiklund O: Oxysterols present in atherosclerotic tissue decrease the expression of lipoprotein lipase messenger RNA in human monocyte-derived macrophages. *J Clin Invest* 1996, 97:461–468
 59. Rowe AH, Argmann CA, Edwards JY, Sawyez CG, Morand OH, Hegele RA, Huff MW: Enhanced synthesis of the oxysterol 24(S),25-epoxycholesterol in macrophages by inhibitors of 2,3-oxidosqualene: lanosterol cyclase. *Circ Res* 2003, 93:717–725